

## Performance evaluation of HHT and WT for detection of HIF and CT saturation in smart grids

Saeid HEIDARI<sup>1,\*</sup> , Saeed ASGHARIGOVAR<sup>1,2</sup> , Pouya POURGHASEM<sup>1</sup> ,  
Heresh SEYEDI<sup>1</sup> , Ömer USTA<sup>2</sup> 

<sup>1</sup>Faculty of Electrical and Computer Engineering, University of Tabriz, Tabriz, Iran

<sup>2</sup>Department of Electrical Engineering, İstanbul Technical University, İstanbul, Turkey

Received: 04.01.2021

Accepted/Published Online: 19.04.2021

Final Version: 23.09.2021

**Abstract:** Hilbert–Huang transform (HHT), continuous wavelet transform (CWT) and discrete wavelet transform (DWT) are well-known signal processing methods that are widely utilized for feature extraction and fault detection by protection systems in smart grids. In this paper, we assess the performances of these methods encountering challenging situations in distribution networks, i.e. high impedance arcing fault (HIF) and current transformer (CT) saturation. Low fault current amplitude in HIF case causes the overcurrent protection, which is the predominant protection method in distribution grids, to fail. Furthermore, some faults may lead to CT saturation, which may result in delayed operation of the relay. To overcome the mentioned problems, researchers employ signal processing approaches such as HHT, DWT or CWT for feature extraction from voltage and current waveforms and import the features to artificial intelligence-based algorithms to detect and discriminate the problems from other normal conditions in power networks. In this regard, HHT, CWT, and DWT are compared under different fault conditions, such as HIF and CT saturation, as well as sudden load increasing, capacitor bank switching, and inrush current of distribution transformers as normal conditions. As a result, simulation studies demonstrate that CWT and DWT are more appropriate for applications of CT saturation and HIF detection in protection of power networks.

**Key words:** Continuous wavelet transform, CT saturation, discrete wavelet transform, feature extraction, high impedance fault, Hilbert–Huang transform

### 1. Introduction

High impedance arcing fault that is generally called high impedance fault (HIF) is a kind of power system disturbance that does not generate enough current to trigger the overcurrent relay [1]. HIF usually occurs for two reasons: either a conductor contacts high impedance objects (e.g., trees and buildings) or a conductor is dropped on a high impedance surface (e.g., roads) [2]. Hence, the possibility of arising this type of fault is high in distribution networks.

HIF is affected by several factors, such as ground material and surface moisture, which are the most significant over other factors [3]. Indeed, augmenting the surface humidity increases the fault current amplitude [4]. Furthermore, HIF may also occur on different materials, which have different voltage-current characteristics [5, 6]. HIF-exposed materials are tree branches, grass, pebbles, sand, asphalt, concrete, and blocks. Unlike most of the power system faults, which primarily endanger electrical equipment, HIF not only may cause to insulation failure and power interruption, but also threatens human safety by possibility of causing fire and

\*Correspondence: s.heidari94@ms.tabrizu.ac.ir

unintentional contacting the conductor [7]. Therefore, since the overcurrent relay may not be able to detect this fault, it must be detected by new algorithms and methods [8].

HIF current integrated with the arc leads to appear several characteristics, which can be helpful in its detecting process and are introduced as follows: a) Current waveform asymmetry: the difference between the positive and negative peak values. b) Build-up: the increasing current of HIF in each cycle to reach the steady state condition. c) Shoulder: stopping the ascending trajectory of the current for a few cycles. d) Nonlinearity: the nonlinear voltage-current characteristic of HIF, due to the arc. Some of these features are shown in Figure 1. Additionally, Figure 2 depicts an Emanuel arc model-based HIF model [4], which is precise and includes all the features of a real HIF. The model consists of six inversed-parallel branches [9–11]. The DC sources are in the range of 1 to 4 kV, and the fault resistance varies from 0.2 to 1.5 kΩ.

Current transformer (CT) saturation is one of the major problems of protection systems, especially the systems that only rely on current signal such as overcurrent protection. It causes the relay to receive the current signal much lower than it is, in a severe saturation condition. Figure 3 illustrates an example of CT saturation condition. Thus, CT saturation may result in the relay mal-operation or delayed operation. The main reasons that the current transformer is saturated are: high fault current, high impedance burden of the relay and residual flux in the core [2]. Hence, its detection plays a prominent role for compensating the distorted current and, consequently, protecting the power network, appropriately.

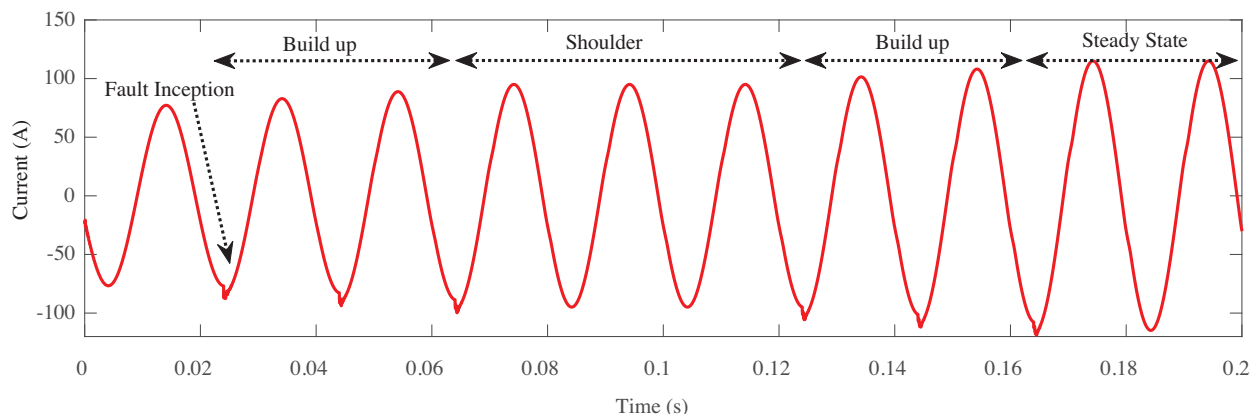


Figure 1. HIF current characteristic.

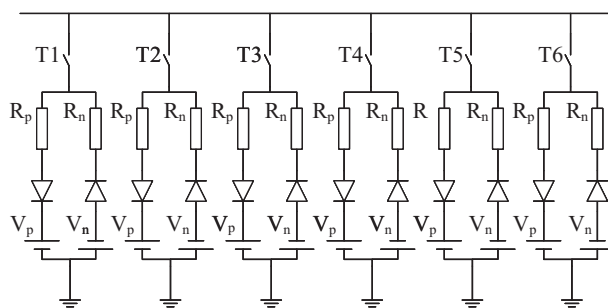
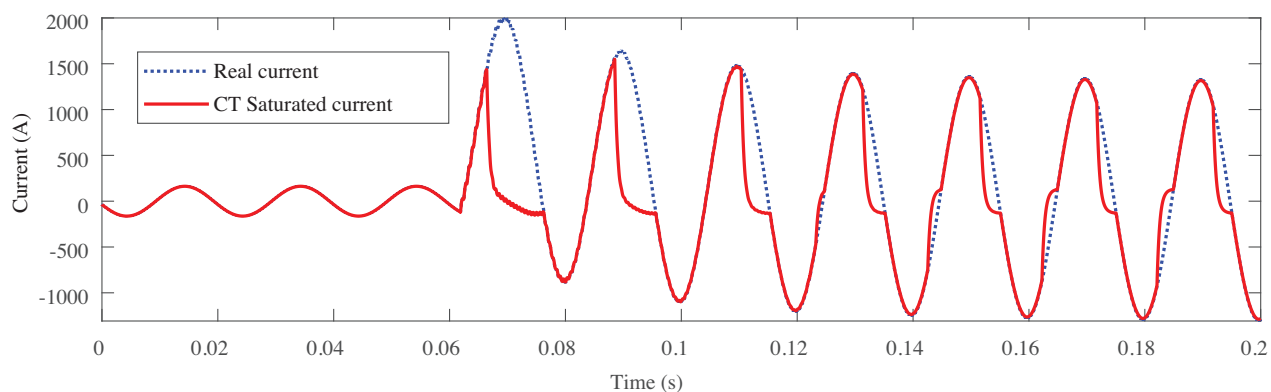


Figure 2. HIF model based on Emanuel arc model.



**Figure 3.** CT saturation effect on current waveform.

In recent years, several research works have utilized Hilbert–Huang transform (HHT) or wavelet transform (WT) for detecting power system faults and disturbances such as HIF and CT saturation. In [3], continuous wavelet transform (CWT) has been employed as a feature extraction scheme to evoke HIF and CT saturation signatures from the current waveforms. Afterwards, extreme learning machine has been exerted to detect and classify the fault conditions. In [5], discrete wavelet transform (DWT) has been applied as a feature extraction approach to detect HIF and discriminate it from insulator leakage current and other transients in power distribution grids. Additionally, WT has been employed to decompose the current signals into their high frequency components to detect HIF in [9, 10]. Furthermore, HHT has been utilized for extracting faults (e.g., HIF) features in [12]. Thereafter, the obtained results have been imported to artificial intelligence approaches to provide a microgrid protection scheme. Moreover, Ref. [13] has proposed an HHT-based HIF detection technique. In this paper, energy of each phase is calculated by intrinsic mode function of three phase currents and voltages to detect the fault. In [14], an HHT based differential approach has been compared to S-transform for HIF detection in microgrids. In [15], DWT has been employed for extracting HIF features. Afterwards, the features have been imported to an evolving neural network for the fault detection. In addition, current signals wavelet coefficients have been utilized for feature extraction application, in [16, 17]

It is obvious that a reliable protection method must be able to not only detect HIF and/or CT saturation, but also discriminate them from normal operating conditions of the power network. Therefore, in this paper, for evaluating HHT and WT performances in the mentioned conditions and discovering the superior method, high frequency information of three-phase current waveforms are extracted by HHT, CWT, and DWT as the main feature in each scenario. In other words, sum of the absolute values of the coefficients ( $S_{COEF}$ ) is computed for one cycle after the fault incidence, initially. This feature is chosen, since it is one of the most simple and informative features that has been utilized in the literature [2, 9]. Afterwards, the results are compared for HIF and CT saturation as fault conditions, and also for sudden load increasing, capacitor bank switching, and inrush current of distribution transformers as normal conditions to identify the premier signal processing method for HIF and CT saturation detection applications.

The remaining sections of the paper are organized as follows. In Section 2, HHT, CWT, and DWT will be introduced. Section 3, is allocated to the comparative study and assessment of HHT, CWT and DWT in different conditions. Section 4 presents the conclusion.

## 2. HHT, CWT, and DWT

HHT, CWT, and DWT are efficient methods in signal processing and are widely used in protection engineering to detect faults in power systems, recently. In this section, we briefly explain their advantages and working procedures.

### 2.1. Hilbert–Huang transform (HHT)

A composition of empirical mode decomposition (EMD) and Hilbert transform (HT) was defined as Hilbert–Huang transform [18]. HHT is a signal processing method that is suitable for nonstationary and nonlinear signals. The significant part of HHT is EMD, which is adaptively able to decompose the input signal to limited number of intrinsic mode functions (IMF). IMFs are appropriate to act as inputs for Hilbert transform. Consequently, HT results in instantaneous frequencies in every instant of time. Therefore, HHT is capable of time-frequency representation of the signal.

From mathematical point of view, HT is defined by the convolution of  $x(t)$  with  $1/t$  as follows:

$$y(t) = (P/\pi) \int_{-\infty}^{+\infty} (x(\tau)/(t - \tau))d\tau, \quad (1)$$

where  $P$  is the basic Cauchy value. By integrating  $x(t)$  with  $y(t)$ , the analytic signal  $z(t)$  is illustrated as Equation 2.

$$z(t) = x(t) + y(t) = a(t)e^{j\phi(t)}, \quad (2)$$

where  $a(t)$  and  $\phi(t)$ , which are instantaneous amplitude and phase of  $x(t)$ , are defined as Equations 3 and 4:

$$a(t) = (x(t)^2 + y(t)^2)^{1/2}, \quad (3)$$

$$\phi(t) = \arctan(y(t)/x(t)). \quad (4)$$

### 2.2. Continuous wavelet transform (CWT)

Wavelet transform is a highly popular technique in signal processing. CWT, which is a linear transform, is one of the methods of wavelet transform and is applied for extracting high frequency information of signals in power system applications. It is defined as follows:

$$C(a, b) = (1/\sqrt{a}) \int_{-\infty}^{+\infty} f(t)\psi((t - b)/a)dt, \quad (5)$$

where  $a$  and  $b$  are the scale and position parameters and  $\psi$  is function of the window, called mother wavelet [2]. The results of this transform are the wavelet coefficients  $C$ , which are functions of scale and location. In simple terms, CWT has been formulated for time-frequency analysis of the input signal. Its advent enhanced the time-frequency analysis, since it solved the problems of short-time Fourier transform. In fact, it determines the time of occurrence of each specific frequency on a nonstationary signal. It also compares the input signal with the selected mother wavelet and investigates their similarities. Therefore, it returns approximately zero for no-fault and normal current signals, whereas, it results high valued coefficients for distorted current signals.

### 2.3. Discrete wavelet transform (DWT)

DWT is a wavelet transform-based signal processing approach, which is widely utilized in feature extraction and fault detection in power systems. It is capable of decomposing nonstationary signals into their low and high frequency components, which are called approximation and detail, respectively. To achieve the approximation and detail, the signal is passed through low pass and high pass filters in each decomposition level. Similar to CWT, it employs a mother wavelet to perform decomposition [19].

### 3. Simulation results

This paper proposes a comparative study among Hilbert–Huang transform, discrete wavelet transform and continuous wavelet transform as three commonly used signal processing methods in protection engineering for detecting high impedance faults and CT saturation and discriminating them from normal operating conditions such as sudden load increasing, capacitor bank switching, and inrush current of distribution transformers. In fact, the main aim of the paper is to distinguish the suitable signal processing or feature extraction technique for HIF and/or CT saturation detection in power systems. In this regard, A 20 kV, 50 Hz, distribution network has been utilized for the simulation studies, as shown in Figure 4. In addition, Table 1 shows the simulated system details in normal operating condition. The sampling frequency is also 100 kHz, thus, there are 2000 samples in each cycle. The fault incidences occur at 0.045 (s). Furthermore, as shown in the figure, the power grid is equipped with a distributed generation (DG) unit, hence, each line requires overcurrent relays at both ends. Nevertheless, we just consider grid side relays (left ones) due to simplicity.

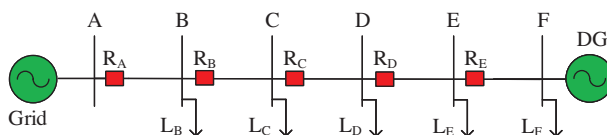


Figure 4. Test distribution system.

Table 1. Load current seen by each relay.

Lines			
Positive sequence resistance ( $\Omega/km$ )	0.01273	Zero sequence resistance ( $\Omega/km$ )	0.3864
Positive sequence inductance ( $H/km$ )	$0.9337e - 3$	Zero sequence inductance ( $H/km$ )	$4.1264e - 3$
Positive sequence capacitance ( $F/km$ )	$12.74e - 9$	Zero sequence capacitance ( $F/km$ )	$7.751e - 9$
Length ( $km$ )	5		
Power grid			
Voltage ( $kV$ )	20	Frequency ( $Hz$ )	50
Short circuit level ( $MVA$ )	100		
Load currents seen by each relay (A)			
$R_A$	240	$R_B$	197
$R_C$	155	$R_D$	114
$R_E$	76		

### 3.1. Case I: CWT, HHT and DWT in HIF condition

In this case, 20 simulations are performed. Indeed, 4 types of HIF with different impedances (from  $HIF_1$  with the minimum impedance to  $HIF_4$  with the maximum impedance) are located in front of each relay and the secondary current of the corresponding CT is obtained for each fault. Thereafter, three-phase current signals are sampled and imported to continuous wavelet transform, Hilbert–Haung transform and discrete wavelet transform. Hence, their high frequency components are achieved. Afterwards, sum of the absolute values of the components ( $S_{COEF}$ ) is calculated for one cycle after the fault incidence for each case. Regarding the mother wavelets of CWT and DWT, we have selected mother wavelets, which produces the minimum coefficients values in normal conditions and generates high coefficients values in fault conditions to obtain the maximum discrimination. Hence, Morlet is selected as mother wavelet of CWT and db4 is used as mother wavelet of DWT with four level decomposition. Figure 5 depicts the currents of  $HIF_1$  to  $HIF_4$  on phase A seen by  $R_A$ . Consequently, Table 2 demonstrates the simulation results. In the table,  $I_{FAULT}$  represents the fault current.

**Table 2.** Simulation results for HIF conditions.

		$HIF_1$	$HIF_2$	$HIF_3$	$HIF_4$
$R_A$	$I_{FAULT}$	666	477	355	274
	$S_{COEF} - CWT$	15639	11289	9944	8869
	$S_{COEF} - HHT$	1.0313e7	6.7586e6	9.0269e6	1.4813e6
	$S_{COEF} - DWT$	34.4567	26.8382	19.2563	12.1014
$R_B$	$I_{FAULT}$	531	411	302	241
	$S_{COEF} - CWT$	9205	7797	6714	5987
	$S_{COEF} - HHT$	3.7921e6	2.0109e6	7.099e5	1.0273e6
	$S_{COEF} - DWT$	61.3840	51.5785	38.4251	25.3725
$R_C$	$I_{FAULT}$	454	349	252	196
	$S_{COEF} - CWT$	6582	5221	4312	3769
	$S_{COEF} - HHT$	3.9593e5	7.1698e4	6.9391e5	5.726e5
	$S_{COEF} - DWT$	39.3122	33.1351	24.6286	15.7937
$R_D$	$I_{FAULT}$	438	319	214	156
	$S_{COEF} - CWT$	4430	3220	3149	2772
	$S_{COEF} - HHT$	4.9433e7	1.7804e7	1.3204e6	8.2918e4
	$S_{COEF} - DWT$	103.1427	87.3787	64.8552	41.0017
$R_E$	$I_{FAULT}$	367	261	167	115
	$S_{COEF} - CWT$	2800	2629	2371	2352
	$S_{COEF} - HHT$	1.0802e7	1.6461e7	1.3416e7	4.6109e6
	$S_{COEF} - DWT$	85.8047	72.917	54.7815	35.5572

As cited in the table,  $S_{COEF}$  of CWT is reduced by increasing the fault impedance (from  $HIF_1$  to  $HIF_4$ ). Its results are in the range of 2325 and 15639. Therefore, CWT is capable of detecting high impedance fault with variety of impedances in different locations. Furthermore, as shown in the table, the sum values of HHT are very large (from 7.1698e4 to 4.9433e7), thus, it is able to detect high impedance fault with different impedances all over the power network. Moreover,  $S_{COEF}$  of DWT is reduced by increasing the fault impedance. Its maximum coefficient is 103.1427 for the fault with the lowest impedance (i.e.  $HIF_1$ ) and the

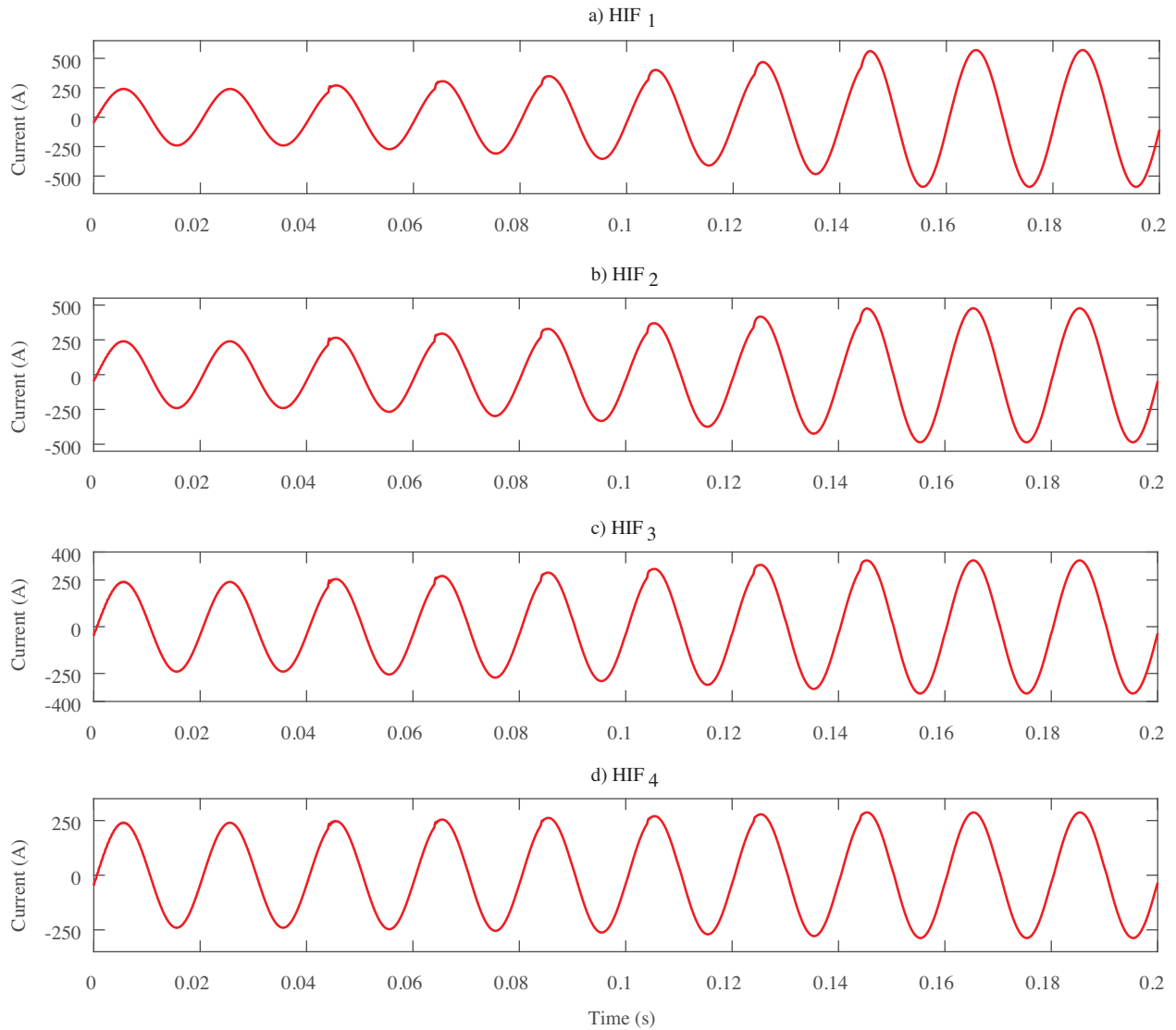


**Figure 5.** Phase A current signal seen by  $R_A$  for a)  $HIF_1$ , b)  $HIF_2$ , c)  $HIF_3$ , d)  $HIF_4$ .

lowest coefficient is 12.1014 for the fault with the highest impedance (i.e.  $HIF_4$ ). Nevertheless, unlike CWT and DWT, whose  $S_{COEF}$  values provide further information about severity or impedance of the fault, HHT is impotent in this regard and there is no meaningful pattern or rule between its results. Indeed, the feature values are not related to the fault impedance.

### 3.2. Case II: CWT, HHT and DWT in CT saturation condition

In this case, 20 simulation studies are implemented. In fact, 4 types of CT saturation with different severities ( $SAT_1$  with higher severity to  $SAT_4$  with lower severity) are simulated in each relay location. Afterwards, distorted secondary current of the corresponding CT is achieved for each case. Thereafter, three-phase current signals are sampled and imported to CWT, HHT, and DWT algorithms. Thus, high frequency components of them are attained. Afterwards, sum of the absolute values of the components ( $S_{COEF}$ ) is computed for one

cycle after the fault occurrence by the output of each method. Figure 6 illustrates current of phase A seen by  $R_A$  for  $SAT_1$  (severe) to  $SAT_4$  (mild) saturation conditions. Moreover, Table 3 shows the simulation results.

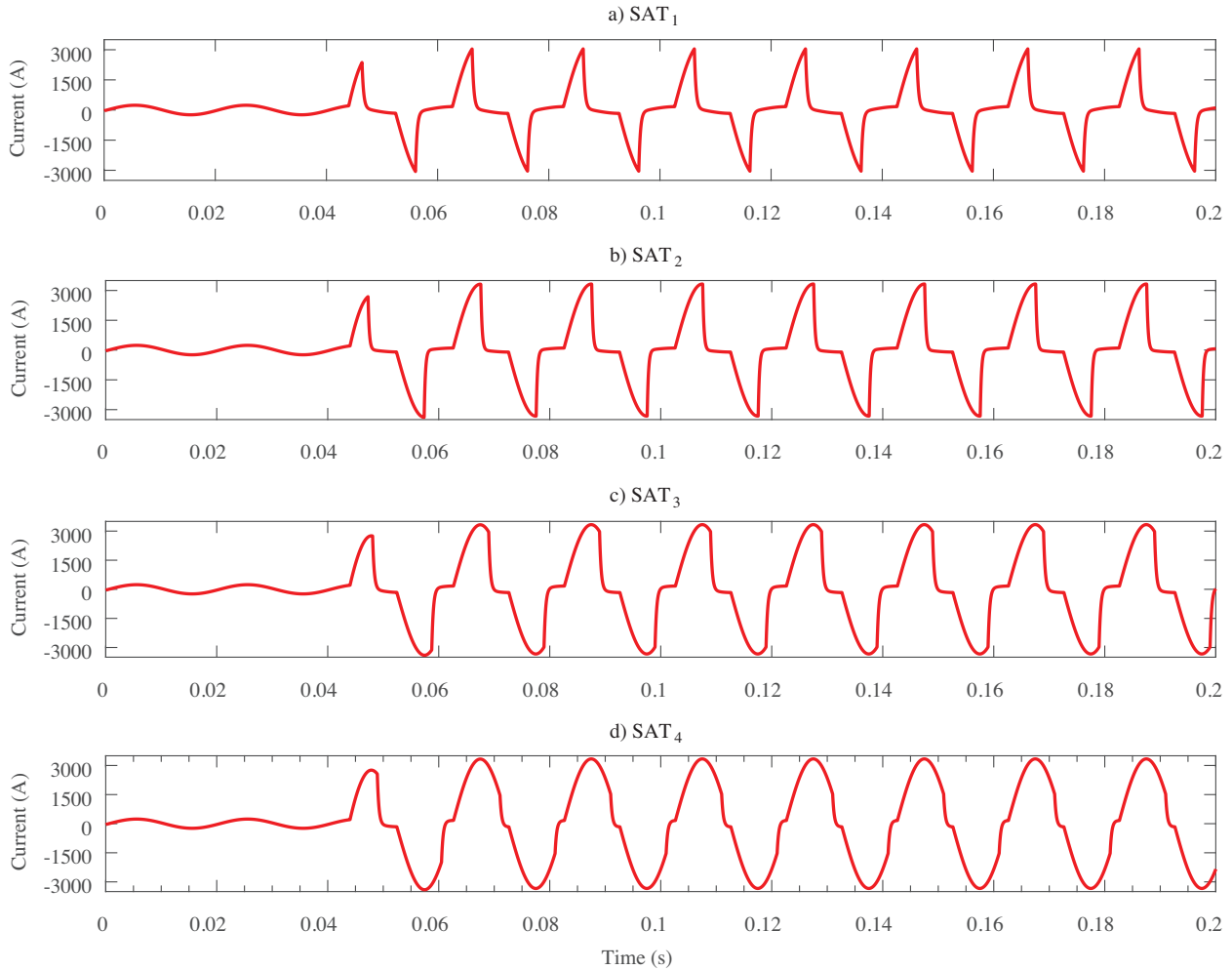


**Figure 6.** Phase A current signal of  $R_A$  for a)  $SAT_1$ , b)  $SAT_2$ , c)  $SAT_3$ , d)  $SAT_4$ .

As stated in the table,  $S_{COEF}$  of CWT is decreased by decreasing the saturation severity. Its results are between 39293 and 734210. Therefore, CWT is able to detect CT saturation with variety of severities in different locations. Furthermore, as is obvious from the table, the coefficient values of HHT are very large (between  $2.449e5$  and  $5.669e8$ ), thus, it is able to detect CT saturation with different severities all over the power network. Moreover, it is observed that the lowest and highest coefficients of DWT for saturation with different severities are 27.8558 and 1081.2. Thus, CT saturation can be easily detected by DWT. Nevertheless, unlike CWT whose  $S_{COEF}$  values provide an approximate information about severity of CT saturation, HHT and DWT are ineffective in this respect and there are no meaningful patterns between their results. In fact, the feature values are not decreased by decreasing the saturation severity.

As a result, CWT is also able to discriminate HIF from CT saturation, since, its maximum  $S_{COEF}$  value of the HIF case (15639) is much smaller than its minimum  $S_{COEF}$  value for the case of CT saturation (39293). Therefore, CWT can be utilized for feature extraction and detection of both cases at the same time in a unique

**Table 3.** Simulation results for CT saturation conditions.

		$SAT_1$	$SAT_2$	$SAT_3$	$SAT_4$
$R_A$	$I_{FAULT}$	3330	3330	3330	3330
	$S_{COEF} - CWT$	734210	704508	700280	442350
	$S_{COEF} - HHT$	8.650e6	1.666e7	2.418e7	1.101e7
	$S_{COEF} - DWT$	1081.2	1331.2	512.240	27.855
$R_B$	$I_{FAULT}$	2600	2600	2600	2600
	$S_{COEF} - CWT$	600610	359570	355960	88535
	$S_{COEF} - HHT$	2.457e8	1.736e7	2.469e5	2.449e5
	$S_{COEF} - DWT$	956.977	1094.6	360.890	202.103
$R_C$	$I_{FAULT}$	2100	2100	2100	2100
	$S_{COEF} - CWT$	494760	79485	77561	67705
	$S_{COEF} - HHT$	5.669e8	7.053e7	1.303e8	2.766e8
	$S_{COEF} - DWT$	737.968	720.183	134.922	125.076
$R_D$	$I_{FAULT}$	1760	1760	1760	1760
	$S_{COEF} - CWT$	405980	105960	63808	45150
	$S_{COEF} - HHT$	4.560e8	2.640e8	2.944e8	2.818e8
	$S_{COEF} - DWT$	629.546	174.069	116.996	91.192
$R_E$	$I_{FAULT}$	1500	1500	1500	1500
	$S_{COEF} - CWT$	330860	63826	51155	39293
	$S_{COEF} - HHT$	7.1e7	2.378e8	8.897e7	1.165e8
	$S_{COEF} - DWT$	383.906	114.716	92.978	77.741

protective relay. However, HHT and DWT are not capable of performing for both HIF and CT saturation cases, simultaneously, as there is an interference between their feature values.

### 3.3. Case III: CWT, HHT and DWT in sudden load increasing

In this section of the simulation studies, impacts of sudden load increasing are investigated and possible interference between  $S_{COEF}$  values of HIF or CT saturation with this condition is perused. In other words, a reliable protection algorithm must be dependable to detect all the faults, while, it must be secure and should not react for normal events like sudden entering a heavy load to the network. In this regard, a simulation study in  $R_A$  relay location is implemented in 6 to 22 percent sudden load increasing conditions. Afterwards, three-phase current waveforms are sampled and imported to CWT, DWT and HHT algorithms. Thus, high frequency components of them are attained and  $S_{COEF}$  values are computed for one cycle after the fault inception by the output of each method. Table 4 expresses the simulation results.

**Table 4.** Simulation results for sudden load increasing conditions in  $R_A$  relay location.

	6%	9%	14%	22%
$S_{COEF} - CWT$	111	114	119	127
$S_{COEF} - HHT$	0	0	0	0
$S_{COEF} - DWT$	1.610e-4	1.542e-4	1.139e-4	1.070e-4

As mentioned in the table, HHT represents ideal results in this case. Indeed, it does not react to sudden load increasing, since its  $S_{COEF}$  values are zero. Although CWT results are not ideal, they are very small (between 111 and 127) and ignorable in comparison with HIF and CT saturation results and there is no interference between them. In addition, DWT coefficients in this case are really small and close to zero. Consequently, all the methods behave appropriately encountering sudden load increasing and successfully discriminate a normal event in the power network from a fault condition.

### 3.4. Case IV: CWT, HHT and DWT in capacitor bank switching

In this section, effects of capacitor bank switching with different capacities are investigated and possible interference between  $S_{COEF}$  values of HIF or CT saturation with this condition is examined. In fact, ideal  $S_{COEF}$  values for such a normal event in distribution system is zero. In this regard, a simulation study is implemented in  $R_A$  relay location for switching 0.5 to 2 MVAR capacitor bank conditions. The capacitors are added to the circuit in 0.04 (s). Figure 7 depicts the current waveforms of the relay during capacitor bank switching procedure. Table 5 announces the simulation results.

**Table 5.** Simulation results for capacitor bank switching conditions in  $R_A$  relay location.

	0.5 MVAR	1 MVAR	1.5 MVAR	2 MVAR
$S_{COEF} - CWT$	1230	674	565	525
$S_{COEF} - HHT$	1.1801e8	7.7858e7	5.7912e6	3.1304e6
$S_{COEF} - DWT$	0.6029	0.5337	0.5128	0.503

As stated in the table,  $S_{COEF}$  value of CWT is decreased by augmenting reactive power of the capacitor bank, because as shown in Figure 7, increasing MVAR of the capacitor causes to decrease the oscillations frequency in current. In addition, CWT  $S_{COEF}$  values are in the range of 1230 to 525, which does not have any interference with  $S_{COEF}$  ranges of HIF or CT saturation. Therefore, CWT does not detect capacitor bank switching as a fault case. Furthermore, as is obvious from the table, the coefficient values of HHT are between 1.180e8 and 3.130e6. Hence, the results have an interference with the fault cases, thus, it incorrectly detects capacitor bank switching as a fault condition. Additionally, the coefficients of DWT are between 0.503 and 0.6029, which can easily be considered as no fault conditions. Therefore, unlike CWT and DWT, which successfully ignore capacitor bank switching, HHT fails in this regard.

### 3.5. Case V: CWT, HHT and DWT encountering inrush current of distribution transformer

In this case, impacts of inrush current of distribution transformer, which is another normal event that frequently occurs in distribution grids, on the signal processing methods performance are evaluated. In this respect, two simulation studies in  $R_A$  relay location are performed during 1 and 2 MVA distribution transformers switching conditions. The transformers are added to the circuit in 0.04 (s). Table 6 shows the simulation results.

As expressed in the table, HHT represents ideal results in this case. Indeed, HHT does not respond to inrush current of transformer, since its  $S_{COEF}$  values are zero. Although results of CWT are not ideal, they are very small (between 856 and 1317) and neglectable in comparison with HIF and CT saturation results and there is no interference between them. Moreover, the coefficients of DWT are very close to zero, which can be easily considered as no fault conditions.

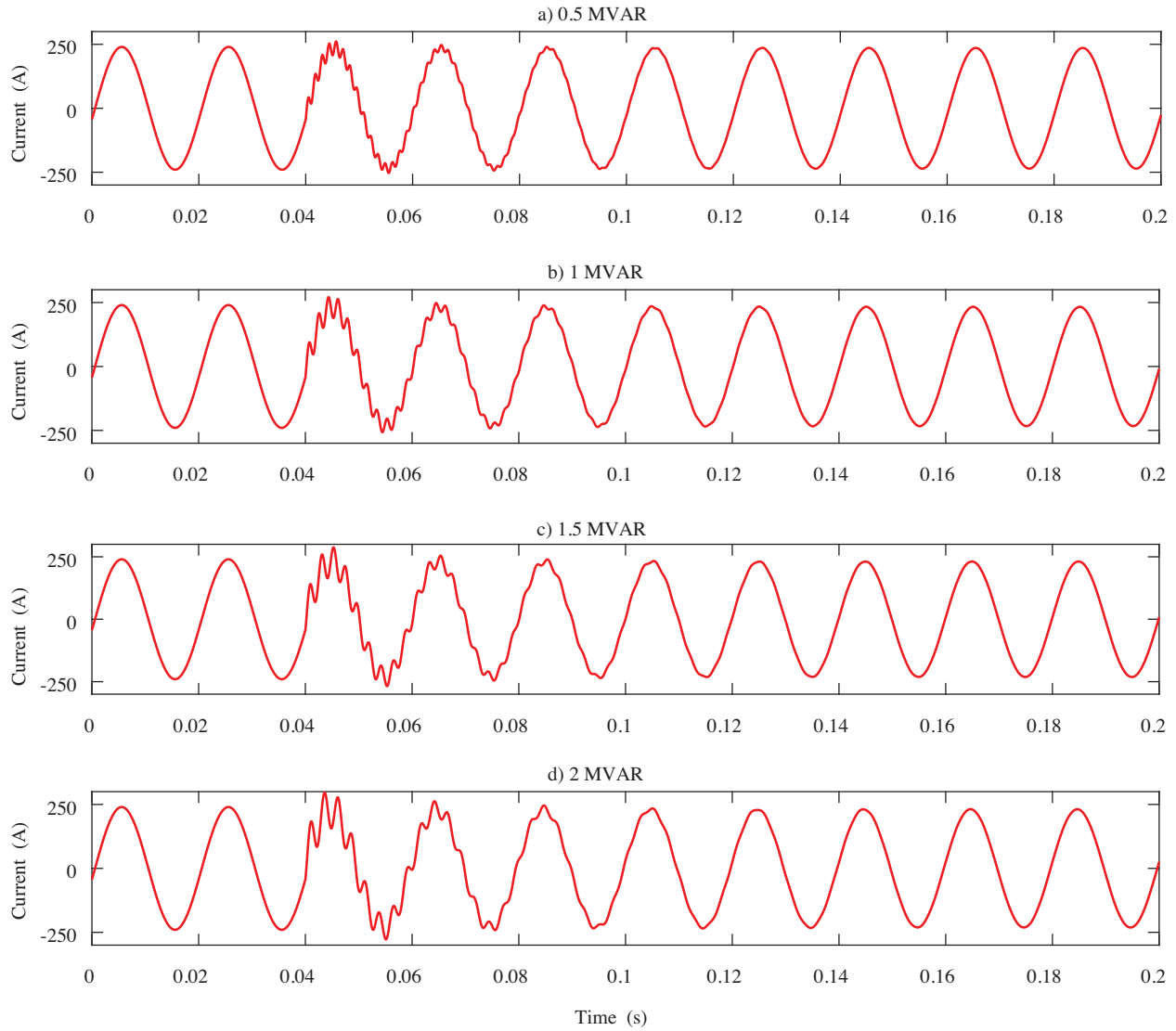


**Figure 7.** Phase A current signal of  $R_A$  for a) 0.5, b) 1, c) 1.5, d) 2 MVAR capacitor bank switching.

**Table 6.** Simulation results for inrush current conditions in  $R_A$  relay location.

	1 MVA	2 MVA
$S_{COEF} - CWT$	856	1317
$S_{COEF} - HHT$	0	0
$S_{COEF} - DWT$	1.6786e-4	1.6786e-4

Therefore, all the methods behave properly facing with transformer inrush current and successfully discriminate this normal event in the power network from a fault condition.

#### 4. Conclusion

In this paper, performances of Hilbert–Huang transform, continuous wavelet transform and discrete wavelet transform are evaluated for feature extraction in HIF protection and CT saturation detection applications. Hence, their capabilities to detect the mentioned fault cases are investigated, initially. Although all methods are successful in detecting the fault conditions, CWT performs better than HHT and DWT. Afterwards, their behavior during normal operating conditions of the distribution network are examined. In this regard, sudden load increasing, capacitor bank switching, and inrush current of transformer are the main challenging cases that may cause to maloperation of protection systems. Thus, we applied the mentioned conditions to the network and monitored the methods performances. In spite of satisfactory performance of HHT for sudden load increasing and inrush current conditions, its results are undesired for capacitor bank switching and they have an interference with HIF and CT saturation results. On the other hand, CWT and DWT perform satisfactory in all normal conditions. In fact, their outputs in normal conditions do not interfere with none of the fault conditions. As a result, CWT and DWT are more suitable than HHT for the applications of HIF and CT saturation detection in smart distribution grids.

#### References

- [1] AsghariGovar S, Seyedi H. A novel transfer matrix-based approach for pilot protection of hybrid transmission lines considering HIF location. *IEEE Transactions on Power Delivery* 2019; 35 (4): 1749-1757. doi: 10.1109/TPWRD.2019.2952538
- [2] AsghariGovar S, Heidari S, Seyedi H, Ghasemzadeh S, Pourghasem P. Adaptive CWT-based overcurrent protection for smart distribution grids considering CT saturation and high-impedance fault. *IET Generation, Transmission & Distribution* 2017; 12 (6): 1366-1373. doi: 10.1049/iet-gtd.2017.0887
- [3] Kim CJ, Russell BD, Watson K. A parameter-based process for selecting high impedance fault detection techniques using decision making under incomplete knowledge. *IEEE Transactions on Power Delivery* 1990; 5 (3): 1314-1320. doi: 10.1109/61.57972
- [4] Emanuel AE, Cyganski D, Orr JA, Shiller S, Gulachenski EM. High impedance fault arcing on sandy soil in 15 kV distribution feeders: contributions to the evaluation of the low frequency spectrum. *IEEE Transactions on Power Delivery* 1990; 5 (2): 676-686. doi: 10.1109/61.53070
- [5] Sedighi AR, Haghifam MR, Malik OP, Ghassemian MH. High impedance fault detection based on wavelet transform and statistical pattern recognition. *IEEE Transactions on Power Delivery* 2005; 20 (4): 2414-2421. doi: 10.1109/TPWRD.2005.852367
- [6] Macedo JR, Resende JW, Bissochi Jr CA, Carvalho D, Castro FC. Proposition of an interharmonic-based methodology for high-impedance fault detection in distribution systems. *IET Generation, Transmission & Distribution* 2015; 9 (16): 2593-2601. doi: 10.1049/iet-gtd.2015.0407
- [7] Aucoin M. Status of high impedance fault detection. *IEEE Transactions on Power Apparatus and Systems* 1985; 637-644. doi: 10.1109/TPAS.1985.318999
- [8] Hamel A, Gaudreau A, Cote M. Intermittent arcing fault on underground low-voltage cables. *IEEE transactions on power delivery* 2004; 19 (4): 1862-1868. doi: 10.1109/TPWRD.2003.822979
- [9] AsghariGovar S, Pourghasem P, Seyedi H. High impedance fault protection scheme for smart grids based on WPT and ELM considering evolving and cross-country faults. *International Journal of Electrical Power & Energy Systems* 2019; 107: 412-421. doi: 10.1016/j.ijepes.2018.12.019
- [10] AsghariGovar S, Seyedi H. Development of PMU-based backup wide area protection for power systems considering HIF detection. *Turkish Journal of Electrical Engineering & Computer Sciences* 2017; 25 (4): 2846-2859. doi: 10.3906/elk-1605-200

- [11] AsghariGovar S, Seyedi H. Adaptive CWT-based transmission line differential protection scheme considering cross country faults and CT saturation. *IET Generation, Transmission & Distribution* 2016; 10 (9): 2035-2041. doi: 10.1049/iet-gtd.2015.0847
- [12] Mishra M, Rout PK. Detection and classification of micro-grid faults based on HHT and machine learning techniques. *IET Generation, Transmission & Distribution* 2017; 12 (2): 388-397. doi: 10.1049/iet-gtd.2017.0502
- [13] Anand A, Affijulla S. Hilbert-Huang transform based fault identification and classification technique for AC power transmission line protection. *International Transactions on Electrical Energy Systems* 2020; 30 (10): e12558. doi: 10.1002/2050-7038.12558
- [14] Gururani A, Mohanty SR, Mohanta JC. Microgrid protection using Hilbert-Huang transform based-differential scheme. *IET Generation, Transmission & Distribution* 2016; 10 (15): 3707-3716. doi: 10.1049/iet-gtd.2015.1563
- [15] Silva S, Costa P, Gouvea M, Lacerda A, Alves F et al. High impedance fault detection in power distribution systems using wavelet transform and evolving neural network. *Electric Power Systems Research* 2018; 154: 474-483. doi: 10.1016/j.epsr.2017.08.039
- [16] Chen J, Phung T, Blackburn T, Ambikairajah E, Zhang D. Detection of high impedance faults using current transformers for sensing and identification based on features extracted using wavelet transform. *IET Generation, Transmission & Distribution* 2016; 10 (12): 2990-2998. doi: 10.1049/iet-gtd.2016.0021
- [17] Chen JC, Phung BT, Wu HW, Zhang DM, Blackburn T. Detection of high impedance faults using wavelet transform. In: *Australasian Universities Power Engineering Conference (AUPEC)*; Perth, WA, Australia; 2014. pp. 1-6.
- [18] Huang NE, Shen Z, Long SR, Wu MC, Shih HH et al. The empirical mode decomposition and the Hilbert spectrum for nonlinear and non-stationary time series analysis. *Proceedings of the Royal Society of London Series A: Mathematical, Physical and Engineering Sciences* 1998; 454 (1971): 903-995. doi: 10.1098/rspa.1998.0193
- [19] Saravanababu K, Balakrishnan P, Sathiyasekar K. Transmission line faults detection, classification, and location using discrete wavelet transform. In: *International Conference on Power, Energy and Control (ICPEC)*; Dindigul, India; 2013. pp. 233-248.